

Testicular cytoprotective effect of glucagon like peptide-1 in diabetic rats involves inhibition of apoptosis, endoplasmic reticulum stress and activation of autophagy

Elshymaa A. Abdel-Hakeem¹, Nagwa M. Zenhom² and Sahar A. Mokhemer³

¹ Department of Medical Physiology, Faculty of Medicine, Minia University, Minia, Egypt

² Department of Medical Biochemistry, Faculty of Medicine, Minia University, Minia, Egypt

³ Department of Histology and Cell Biology, Faculty of Medicine, Minia University, Minia, Egypt

Abstract. This study aimed to explore the possible cytoprotective effects of exenatide, a glucagon-like peptide-1 (GLP-1) receptor agonist, in the testicles of diabetic rats. Exenatide has numerous advantageous properties in addition to its hypoglycemic effect. However, its impact on testicular tissue in diabetes needs more clarification. Therefore, rats were divided into control, exenatide-treated, diabetic and exenatide-treated diabetic groups. Blood glucose and serum levels of insulin, testosterone, pituitary gonadotropins and kisspeptin-1 were measured. Real-time PCR for beclin-1, p62, mammalian target of rapamycin (mTOR), and AMP-activated protein kinase (AMPK), were estimated in testicular tissue in addition to markers of oxidative stress, inflammation, and endoplasmic reticulum stress. Also, immuno-expression of protein P53, nuclear erythroid factor2 (Nrf2) and vimentin was conducted. Exenatide was able to attenuate diabetic toxic changes and enhance autophagy in testicular tissue. These results indicate the protective effect of exenatide against diabetic testicular dysfunction.

Key words: GLP-1 — Exenatide — Diabetes — Testicular dysfunction — Autophagy — AMPK

Introduction

Diabetes is well-known to cause male reproductive dysfunctions which results in infertility. Reduced testicular functions were widely detected in hyperglycemic animals and diabetic humans. It was documented that spermatogenesis, sperm count, motility and testosterone levels are lower in diabetic individuals as compared to healthy ones (Maresch et al. 2017). All the levels of the male reproductive system seem to be affected by the harmful effects of diabetes. In fact, diabetes was documented to affect not only testicular functions, but also the hypothalamo-pituitary-gonadal axis (HPG) (Tavares et al. 2018).

Multiple intermingled mechanisms share in the detrimental effects of diabetes on the testes, including oxidative stress, inflammation, apoptosis (Barkabi-Zanjani et al. 2020) and recently, there is curiosity to highlight the role of autophagy and endoplasmic reticulum stress (ERS) in the diabetic milieu which needs more clarification.

The age of patients suffering from diabetes-induced reproductive dysfunction is becoming younger. Therefore, it is critical to investigate the mechanisms involved in diabetic testicular dysfunction and to discover new ways to protect male reproductive health.

Glucagon-like peptide-1 (GLP-1) is an incretin hormone that causes higher insulin sensitivity to glucose, insulin release and normalization of elevated glucose levels (Elbasuoni 2014). These effects are mediated by the activation of the glucagon-like receptor (GLP-1R) in pancreatic β -cells (Barakat et al. 2016). Notably, it is now documented that GLP-1R is expressed in a variety of tissues other than the pancreas, providing strong evidence for its extra-pancreatic

Correspondence to: Elshymaa Abdel-Hady Abdel-Hakeem, Medical Physiology Department, Faculty of Medicine, Minia University, 61111 Minia, Egypt
E-mail: shady@mu.edu.eg
shymaa_hady2006@yahoo.com

effects. GLP-1 has a well-documented anti-apoptotic and potent anti-inflammatory role in many tissues. These properties merit significant consideration in the non-metabolic actions of this peptide (Pujadas and Drucker 2016).

Exenatide is a GLP-1 agonist that is approved as an anti-diabetic drug. Exenatide binds to and activates GLP-1 receptors in organs other than the pancreas, including the heart, gut, hypothalamus, and kidney (Ban et al. 2008; Wang et al. 2019) and it was recently discovered in the testes (Caltabiano et al. 2020). In addition to its ability to control blood glucose, exenatide has anti-oxidant, anti-inflammatory and apoptosis inhibitory effects. However, little is known about its role in reproductive organs and testicular dysfunction in diabetes, which needs further illumination (Chang et al. 2014). Therefore, our study aimed to shed light on the possible cytoprotective effects of exenatide in the testicles of diabetic rats and to explore the associated mechanisms, focusing on the role of ERS and autophagy.

Materials and Methods

Animals

Adult male albino rats (8–10 weeks) weighing between 220–250 g were used in this work. Rats were housed in our animal facility unit at room temperature with natural light/dark cycle which was approximately 12 h/12 h, and allowed to eat a standard diet of rat chow and provided water *ad libitum*. Animals were left to acclimatize to the environment for 2 weeks before being included in this work.

Induction of type II diabetes mellitus in rats

The rats were allocated into two dietary regimens by feeding either a normal pellet diet (NPD) to the control rats or a high

fat diet (HFD) (58% fat, 25% protein and 17% carbohydrate, as a percentage of total kcal) for the induction of diabetic rats. Diet composition followed that of Habib et al. (2021).

After 2 weeks of HFD, rats received a low dose of streptozotocin at a dose level of 35 mg/kg after an overnight fast to induce type 2 diabetes. Verification of diabetes was done after 72 h and rats having a blood glucose level ≥ 200 mg/dl were considered diabetic and included in this study. Both dietary regimens continued till the end of the experiment.

Exenatide's treatment protocol

Administration of exenatide (Eli Lilly Company, USA) was initiated 4 weeks after confirmation of diabetes and lasted for another 4 weeks. Exenatide was dissolved immediately in normal saline just before injection and was given at a dose level of 5 μ g/kg/day single subcutaneous (SC) injection (Elbassuoni 2014). The control group and the diabetic non-treated group received the same volume of saline solution every day, so treatment of either saline or exenatide started 4 weeks after confirmation of diabetes and continued for 4 weeks. The experimental rats were separated into four groups of ten rats in each.

C group: control rats were injected SC with saline for 4 weeks before being euthanized.

C+EXT group: control rats were injected with exenatide for 4 weeks before being euthanized (Elbassuoni 2014).

D group: diabetic rats in which induction of diabetes was achieved as mentioned before. Rats of this group received saline injections 4 weeks after verification of diabetes and continued for 4 weeks (Habib et al. 2021).

D+EXT group: rats were treated with exenatide 4 weeks after verification of diabetes and continued for 4 weeks (Habib et al. 2021). Treatment was given at the same time every day.

The experimental timeline and drug regimen are illustrated in Figure 1.

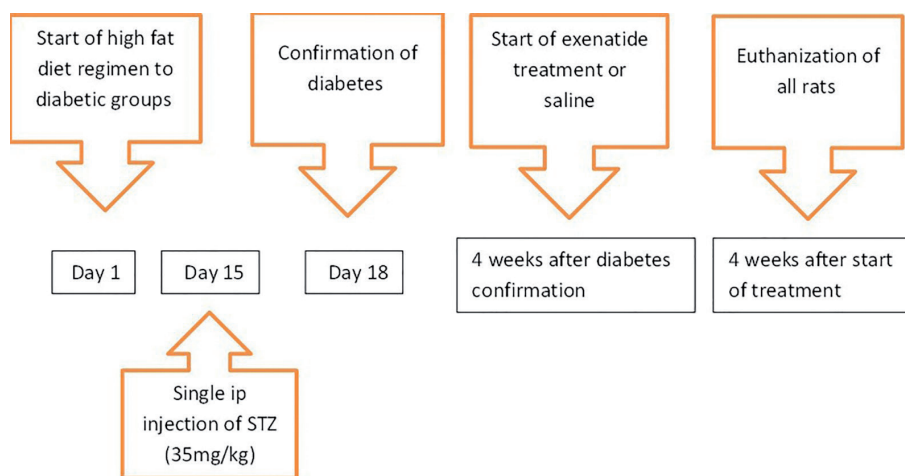


Figure 1. Experimental timeline and drug regimen used during the study period. A high fat diet with a single intraperitoneal injection of a low dose of streptozotocin (STZ, 35 mg/kg) was used to induce type 2 diabetes in rats. Treatment with either exenatide or saline started 4 weeks after confirmation of diabetes and continued for another 4 weeks, after which all rats were euthanized.

Samples collection

All animals were euthanized under light ether anesthesia by decapitation 24 h after the last treatment dose. Blood samples were gathered and left to clot at room temperature, then centrifuged at 3,000 rpm for 15 min. The clear sera were carefully collected, placed in clean labeled containers and kept at -20°C till time of analysis.

The testes and epididymis of each animal were dissected and collected. One testis of each rat was fixed in Bouin's fluid for 24 h for histopathological examination. The other testis was snap-frozen in liquid nitrogen and kept at -80°C for RT-PCR and further biochemical analyses.

Epididymal sperm count and motility

The sperm count was estimated using a hemocytometer. In brief, the cauda epididymis of each rat was carefully separated and minced without delay in 5 ml of physiological saline, then incubated at 37°C for 30 min to let sperms leave the epididymal tubules. An ordinary microscope at $\times 400$ magnification was used to estimate the percentage of motile sperms. The sperms' total number was measured as the count of sperms *per ml* (Heeba and Hamza 2015; Nazmy et al. 2019).

Estimation of serum follicle-stimulating hormone (FSH), luteinizing hormone (LH), testosterone and kisspeptin levels

Serum levels of FSH, LH, and testosterone were measured using ELISA Kits (DRG Instruments GmbH, Marburg, Germany). Serum kisspeptin level was evaluated by using Kisspeptin ELISA Kit. (Cusabio Biotech, Wuhan, China). All measurements were conducted according to the manufacturer's instructions.

Estimation of blood glucose and insulin and estimation of HOMA-IR

Fasting blood glucose level was measured by One-Touch glucometer and fasting serum insulin level was measured using ELISA Kit (Thermo Fisher scientific, USA) following the manufacturer's instructions. Insulin resistance was evaluated by calculating homeostasis model assessment for insulin resistance (HOMA-IR) using the following formula: $\text{HOMA-IR} = \text{glucose concentration (mg/dl)} \times \text{insulin } (\mu\text{U/ml}) / 405$ (Mari et al. 2005).

Testicular tissue analysis

Specimens from each testis were weighed and homogenized in ice-cold phosphate-buffered saline (PBS; pH 7.4). The homogenates were centrifuged at 5,000 rpm for 10 min. The

resultant supernatants were used for estimation of malondialdehyde (MDA), total antioxidant capacity (TAC), TNF- α , IL-10, B-cell leukemia/lymphoma-2 (Bcl-2), Bax, caspase-12 and C/EBP-homologous protein (CHOP).

Determination of MDA, the marker of lipid peroxidation, was based on its reaction with thiobarbituric acid in acidic medium at a temperature of 95°C for 30 min to form a pink complex with an absorption maximum at 534 nm (Ohkawa et al. 1979).

Assay of TAC was done using a Colorimetric Assay Kit (Biodiagnostic, Egypt). Bcl-2 (Life span Biosciences, USA), Bax, caspase-12, CHOP (MyBiosource, San Diego, USA), TNF- α (Lab Vision Corporation, USA) and IL-10 (Cusabio Biotech Co, China) were measured using ELISA Kits as directed by the manufacturer.

Real-time reverse transcription polymerase chain reaction for the relative quantification of beclin-1, AMPK, p62 and mTOR

Total RNA was extracted from homogenized testicular specimens using Trizol RNA extraction reagent (Life Technologies, USA) following the manufacturer's instructions.

cDNAs were synthesized using revert aid™ first strand cDNA synthesis kit (Fermentas, Life Sciences). cDNA was reversely transcribed from 5 μg of mRNA in transcription buffer, 200 U M-MuLV reverse transcriptase, 20 U RNase inhibitor at 42°C for 60 min followed by immediate cooling on ice. Real-time polymerase chain reaction (RT-PCR) was performed with 50 ng cDNA *per* reaction using 25 μl of SYBR green QPCR mix (Solis BioDyne) containing 20 μM of specific primers in the RT-PCR detection system. The SYBR green data were analyzed with a relative quantification to GAPDH (glyceraldehyde-3-phosphate dehydrogenase) as reference gene. The sets of primers used were as follow:

Rat beclin-1 sense primers; 5'-TGAGGGATGGAA-GGGTCTAAG-3', and antisense, 5'-GCCTGGGCTGTG-GTAAGTAATC-3; Rat AMPK sense primers; 5'- AGA-TAGCTGACTTCGGACTCTCT-3' and antisense, 5'- AAC-CTCAGGACCCGCATACA-3'; Rat mTOR, sense primers; 5'-TTGCCAACTACCTTCGGAACC-3' and antisense, 5'-TCA CGGAGAACGA GGACAGC-3'; Rat p62 sense primers; 5'-GGAAGTATGGAGTCGGATAAC-3' and antisense, 5'-GTGGATGGGTCCACTTCTTT-3'; GAPDH sense primers: 5' GTCGGTGTGAACGGATTTG3' and antisense, 5' CTTGCCGTGGGTAGAGTCAT3'. The relative expression level of each gene was calculated using the formula $2^{-\Delta\Delta\text{Ct}}$ according to VanGuilder and colleagues (VanGuilder et al. 2008).

They were scaled relative to the control where control samples were set at a value of 1. Thus, results for all experimental samples were graphed as relative expression compared with the control group.

Tissue preparation for histopathological studies

Testes fixed in Bouin's solution were transferred to 70% ethanol and maintained it until processed using the traditional way to dehydrate in ascending grades of alcohol and clearing by pure xylene. The testes were then embedded in paraffin, sectioned transversally (4 μ m thickness), mounted on glass slides, deparaffinized and rehydrated, and processed for hematoxylin and eosin (H&E) (Suvarna et al. 2018) and immuno-histochemical studies.

Immuno-histochemical study

Testicular sections were immuno-stained for P53 (pro-apoptotic molecule), Nrf2 (antioxidant molecule) and vimentin (sertoli cell marker) according to the manufacturer's instructions. In brief, sections were deparaffinized and rehydrated then endogenous peroxidase activity was blocked using 0.01% hydrogen peroxide. Sections were submerged in trypsin for antigen retrieval and blocking of nonspecific background staining was performed using normal goat serum (1:50). Sections were incubated at 4°C overnight with the primary antibodies; anti-P53 (polyclonal, Catalog Number; ab131442, at a concentration of 1/100 (Abcam Co.), anti-Nrf2 (polyclonal, Catalog Number; PA5-27882, at a concentration of 1/500 (Thermo fisher Co.) and anti-vimentin (polyclonal, Catalog Number; ab137321, at a concentration of 1/200 (Abcam Co.). After a PBS rinse, sections were developed with a secondary antibody HRP kit (DAKO) for 15–20 min, then washed and put in a peroxidase substrate (DAB) solution for 15 min. Tissue sections were last counterstained with hematoxylin.

Morphometric analysis

In H&E-stained sections, the mean seminiferous tubule diameter, lumen diameter, and germinal epithelium height were measured. All previous measures were obtained from round or nearly round cross-sections of seminiferous tubule in four different regions and then the mean value was calculated. The mean area fraction and optical densities of

anti-P53 and anti-vimentin immuno-positive expression were assessed. Additionally, the mean numbers and optical densities of anti-Nrf2 positive nuclear expression were assessed.

All previously mentioned morphological parameters were assessed at 400 magnification in ten adjacent non-overlapping fields from each rat in all groups ($n = 10$). The histologist was blinded to the different experimental groups.

Image acquisition was performed using an Olympus digital camera (LC20, Germany), which was coupled to a BX51 light microscope (Olympus, Japan). For image analysis, ImageJ software (<http://rsbweb.nih.gov/ij/>; NIH, Bethesda) was used.

Statistical analysis

The data of our results were presented as a mean \pm standard error of the mean (SEM) and were statistically analyzed using one-way analysis of variance (ANOVA) followed by Tukey's multiple comparison tests. The analyzing software was GraphPad Prism Program (version 7). Statistical significance was considered when the p value ≤ 0.05 .

Results

Evaluation of blood glucose, insulin and HOMA-IR level in different groups

As shown in Table 1, induction of diabetes evoked significant hyperglycemia and hypoinsulinemia with increased HOMA-IR when compared to the control group. Administration of exenatide reversed these effects and caused a significant reduction in both blood glucose level and HOMA-IR, whereas serum insulin level was raised towards normal.

Evaluation of epididymal sperm count and sperm motility

The D group revealed a significant decrease in sperm count and motility when compared to the control one, whereas

Table 1. Blood glucose, serum insulin and HOMA-IR index in different groups

Parameter	Group			
	C	C+EXT	D	D+EXT
Glucose (mg/dl)	79.3 \pm 2.1 ^b	77.7 \pm 2.24 ^b	312 \pm 9.7 ^a	96.7 \pm 2.17 ^b
Insulin (μ IU/ml)	7.58 \pm 0.53 ^a	7.35 \pm 0.51 ^a	5.24 \pm 0.19 ^b	8.1 \pm 0.48 ^a
HOMA-IR	1.46 \pm 0.08 ^c	1.41 \pm 0.11 ^c	4.03 \pm 0.16 ^a	1.93 \pm 0.12 ^b

Data represent mean \pm SEM of 10 observations. Means in the same horizontal raw having different letters (^{a,b,c}) are significantly different ($p \leq 0.05$). C, control; C+EXT, control treated with exenatide; D, diabetic; D+EXT, diabetic treated with exenatide; HOMA-IR, homeostasis model assessment for insulin resistance.

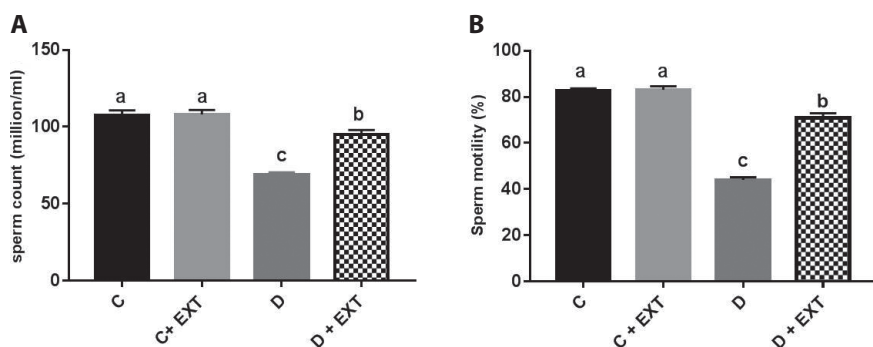


Figure 2. Sperm count (A) and sperm motility (B) in different groups. Values of 10 rats in each group are presented in the form of mean ± SEM. Means having different letters (^{a,b,c}) are significantly different ($p \leq 0.05$). C, control; D, diabetic; C+EXT, control treated with exenatide; D+EXT, diabetic treated with exenatide.

D+EXT group showed a significant increase in sperm count and motility compared to the D group, but their levels were still significantly different from the C group (Fig. 2).

Evaluation of serum level of pituitary gonadotropins, testosterone and kisspeptin level in different groups

Diabetic rats showed a significant reduction in the serum levels of pituitary gonadotropins (FSH and LH), testosterone and kisspeptin when compared to control rats. On the contrary, D+EXT group revealed a significant increase in these hormonal levels when compared to D group (Table 2).

Evaluation of testicular oxidative and inflammatory status

Diabetic rats had higher MDA and TNF-α testicular levels and lower TAC and IL-10 levels when compared to control rats. D+EXT group showed reduced both testicular MDA and TNF-α level while increasing testicular TAC and IL-10 (Table 3).

Evaluation of testicular apoptotic and endoplasmic reticulum stress (ERS) markers

As shown in Figure 3, induction of diabetes resulted in elevated ERS markers, CHOP and caspase-12, along with the proapoptotic Bax. Meanwhile, a reduction of the antia-

Table 2. Hormonal assay in different groups

Parameter	Group			
	C	C+EXT	D	D+EXT
FSH (mIU/ml)	1.59 ± 0.068 ^a	1.70 ± 0.10 ^a	0.68 ± 0.067 ^c	1.12 ± 0.060 ^b
LH (mIU/ml)	1.037 ± 0.09 ^a	0.98 ± 0.088 ^a	0.35 ± 0.04 ^{9c}	0.69 ± 0.03 ^b
Testosterone (ng/ml)	4.81 ± 0.32 ^a	5.18 ± 0.47 ^a	2.01 ± 0.16 ^c	3.52 ± 0.22 ^b
Kisspeptin (ng/ml)	1.77 ± 0.12 ^a	1.78 ± 0.14 ^a	0.98 ± 0.08 ^b	1.57 ± 0.096 ^a

Data represent mean ± SEM of 10 observations. Means in the same horizontal raw having different letters (^{a,b,c}) are significantly different ($p \leq 0.05$). FSH, follicle stimulating hormone; LH, luteinizing hormone. For more abbreviations, see Table 1.

Table 3. Testicular tissue oxidative and inflammatory parameters in different groups

Parameters	Group			
	C	C+EXT	D	D+EXT
MDA (nmol/mg tissue)	15.13 ± 0.52 ^b	13.63 ± 0.31 ^c	40.27 ± 0.56 ^a	16.4 ± 0.53 ^b
TAC (µm/mg tissue)	9.04 ± 0.25 ^a	9.14 ± 0.28 ^a	4.69 ± 0.22 ^b	9.27 ± 0.32 ^a
TNF-α (pg/mg tissue)	22.26 ± 0.98 ^c	19.08 ± 0.97 ^c	47.01 ± 1.52 ^a	31.18 ± 1.1 ^b
IL-10 (pg/mg tissue)	93.67 ± 2.78 ^a	94.89 ± 2.80 ^a	67.78 ± 1.22 ^c	83.85 ± 1.71 ^b

Data represent mean ± SEM of 10 observations. Means in the same horizontal raw having different letters (^{a,b,c}) are significantly different ($p \leq 0.05$). MDA, malondialdehyde; TAC, total antioxidant capacity; TNF-α, tumor necrosis factor alpha; IL-10, interleukin-10. For more abbreviations, see Table 1.

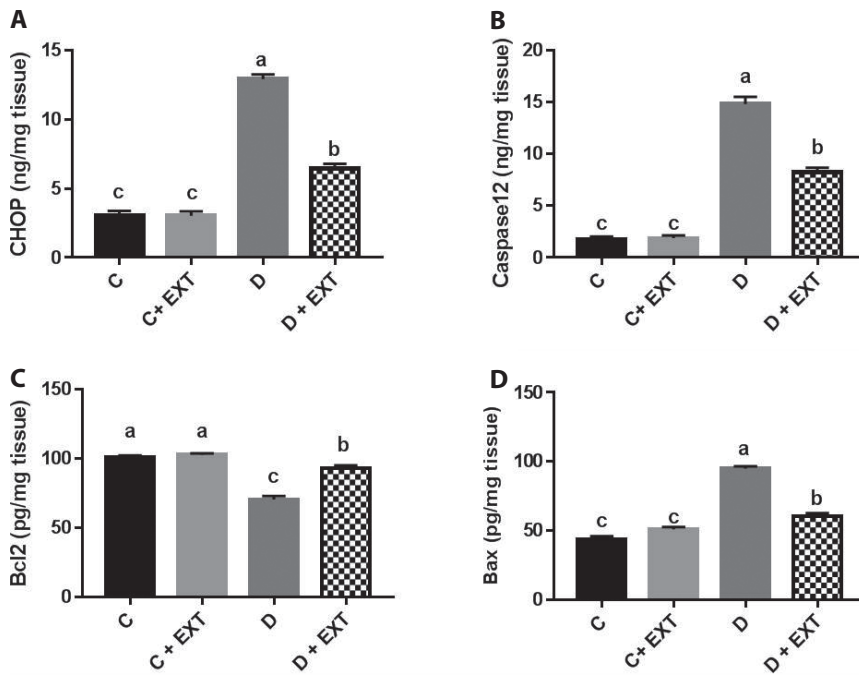


Figure 3. Endoplasmic stress markers CHOP (A), caspase-12 (B), and apoptotic markers Bcl-2 (C), Bax (D) in different groups. Values of 10 rats in each group are presented in the form of mean \pm SEM. Means having different letters (a,b,c) are significantly different ($p \leq 0.05$). For abbreviations, see Figure 2.

apoptotic molecule Bcl-2 was observed. However, the D+EXT group showed significant decrease in ERS markers and elevation of Bcl-2 when compared to the D group.

RT-PCR relative gene expression of AMPK, mTOR, p62 and beclin-1 in testicular tissue

Induction of diabetes resulted in significant down-regulation of AMPK mRNA and beclin-1 mRNA, whereas mTOR and p62 mRNA were enhanced when compared to the control group. Administration of exenatide to diabetic rats significantly up-regulated both AMPK and beclin-1 mRNA expression and decreased the expression of mTOR and p62 mRNA towards the control level (Fig. 4).

Hematoxylin & eosin (H&E) results

As shown in Figure 5, microscopic examination of testicular tissues from both control (Fig. 5A,B) and C+EXT (Fig. 5C,D) groups revealed normal histological architecture of the seminiferous tubules with intact interstitial tissues containing leydig cells and blood vessels. The seminiferous tubules were lined with germinal epithelium including sertoli cells with basally located vesicular nuclei and several rows of spermatogenic cells at various stages of maturation, including spermatogonia resting on the basal lamina, 1ry spermatocytes containing large nuclei with dark chromatin clumps, 2ry spermatocytes, spermatids with rounded nuclei, late spermatids with dense elongated nuclei and sperms in the tubules' lumina. Intact basal lamina and myoid cells

were also noticed. The D group (Fig. 5E-G) showed distortion of seminiferous tubules' architecture, some tubules were atrophied with germinal epithelium depletion; others showed empty spaces within the germinal epithelium, cellular sloughing or separation from basal lamina with irregular or even discontinuous basal lamina. Damaged sertoli cells with disrupted cytoplasmic extensions as well as pyknosis and karyolysis of spermatogenic cells were also noticed. The interstitial tissue revealed deposition of acidophilic vacuolated hyaline material, degenerated leydig cells and vascular congestion with extravascular migration of neutrophils. The D+EXT group (Fig. 5H,I) showed restoration of the germinal epithelium with normal seminiferous tubules' architecture. Spermatogenic cells at the different stages of maturation, sertoli cells, basal lamina, and leydig cells appeared normal. Tubules with minimal germinal epithelium separation from the basal lamina and interstitial hyaline deposition were also observed. Morphometric analysis showed significant decrease in both tubule diameter and epithelial height with significant increase in lumen diameter in D group when compared to control groups (Fig. 5J). However, D+EXT group showed a significant increase in tubular diameter and epithelial height with a significant decrease in lumen diameter when compared to the D group.

Immuno-histochemical results for P53, Nrf2 and vimentin expression

Immuno-histochemical staining for P53 showed negative expression in both control and C+EXT groups. D group

showed a significant increase in both mean area fraction and optical densities of anti-P53 immuno-positive expression in germinal epithelium and leydig cells when compared to the control groups. The D+EXT group revealed a significant decrease in these parameters when compared to the D group, located mainly in sertoli and leydig cells (Fig. 6).

Regarding Nrf2 immuno-expression, germinal epithelium and leydig cells in the control and C+EXT groups revealed a positive expression, mainly cytoplasmic. The D group showed a significant decrease in both mean numbers and optical densities of anti-Nrf2 positive nuclear expression compared to control groups. However, D+EXT group showed a significant increase in these parameters compared not only to D group, but also to control groups, with obvious Nrf2 nuclear accumulation in the germinal epithelium (Fig. 7).

As regards vimentin expression, the control and C+EXT groups showed sertoli cells with characteristic strong positive vimentin distribution radiating toward the tubules' lumina. On the other hand, the D group showed a significant decrease in both mean area fraction and optical densities of vimentin expression compared to C groups. D+EXT group showed significantly improved vimentin expression as compared to the D group (Fig. 8).

Discussion

Male reproductive dysfunction induced by diabetes is still an important issue that deserves more attention. Accordingly,

this study was designed to evaluate the possible testicular cytoprotective effect of the GLP-1 analogue, exenatide, in diabetic rats and investigate the underlying mechanisms that could be involved. To address this point, we chose to induce a type II diabetic animal model of HFD and low dose STZ to mimic human type 2 diabetes (T2DM). This model was confirmed in previous studies with hyperglycemia and increased insulin resistance as seen in our study (Srinivasan et al. 2005; Gheibi et al. 2017).

Diabetes is well-known to affect testicular structure and function. In our study, we found marked deterioration in both the endocrine and spermatogenic functions of the testes in our study evidenced by a significant reduction in sperm count, motility, and serum testosterone level. In addition, there was a marked alteration in testicular architecture seen in the microscopic examination and decreased vimentin immuno-expression, denoting disruption of the sertoli cell barrier, which is mandatory for proper spermatogenic function. Notably, there was a reduction in serum pituitary gonadotropins (LH and FSH) and kisspeptin (Kiss) levels as detected by other researchers (Castellano et al. 2006; Asare-Anane et al. 2019).

Low endogenous Kiss secretion was reported as one of the metabolic and endocrine pathways in the progression of testosterone deficiency and complications seen in T2DM (Daka et al. 2015; Asare-Anane et al. 2019). Here, administration of exenatide to diabetic rats improved serum testosterone, pituitary gonadotropins and Kiss levels. These results are consistent with previous studies such as that of Hany et al. (2018) who reported that GLP-1 injec-

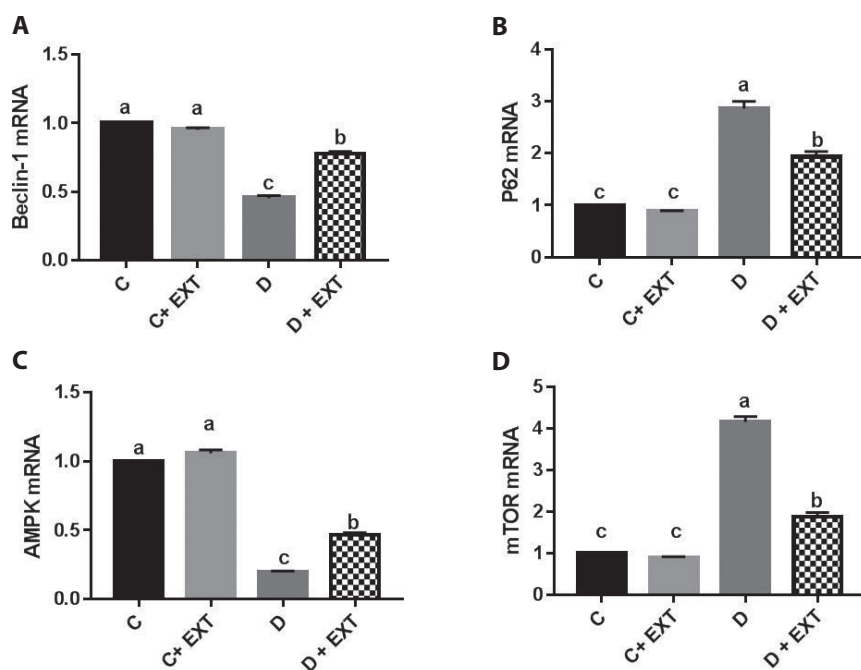


Figure 4. Relative gene expression of beclin-1 (A), p62 (B), AMPK (C), and mTOR (D) in different groups. Values of 10 rats in each group are presented in the form of mean \pm SEM. Means having different letters (^{a,b,c}) are significantly different ($p \leq 0.05$). For abbreviations, see Figure 2.

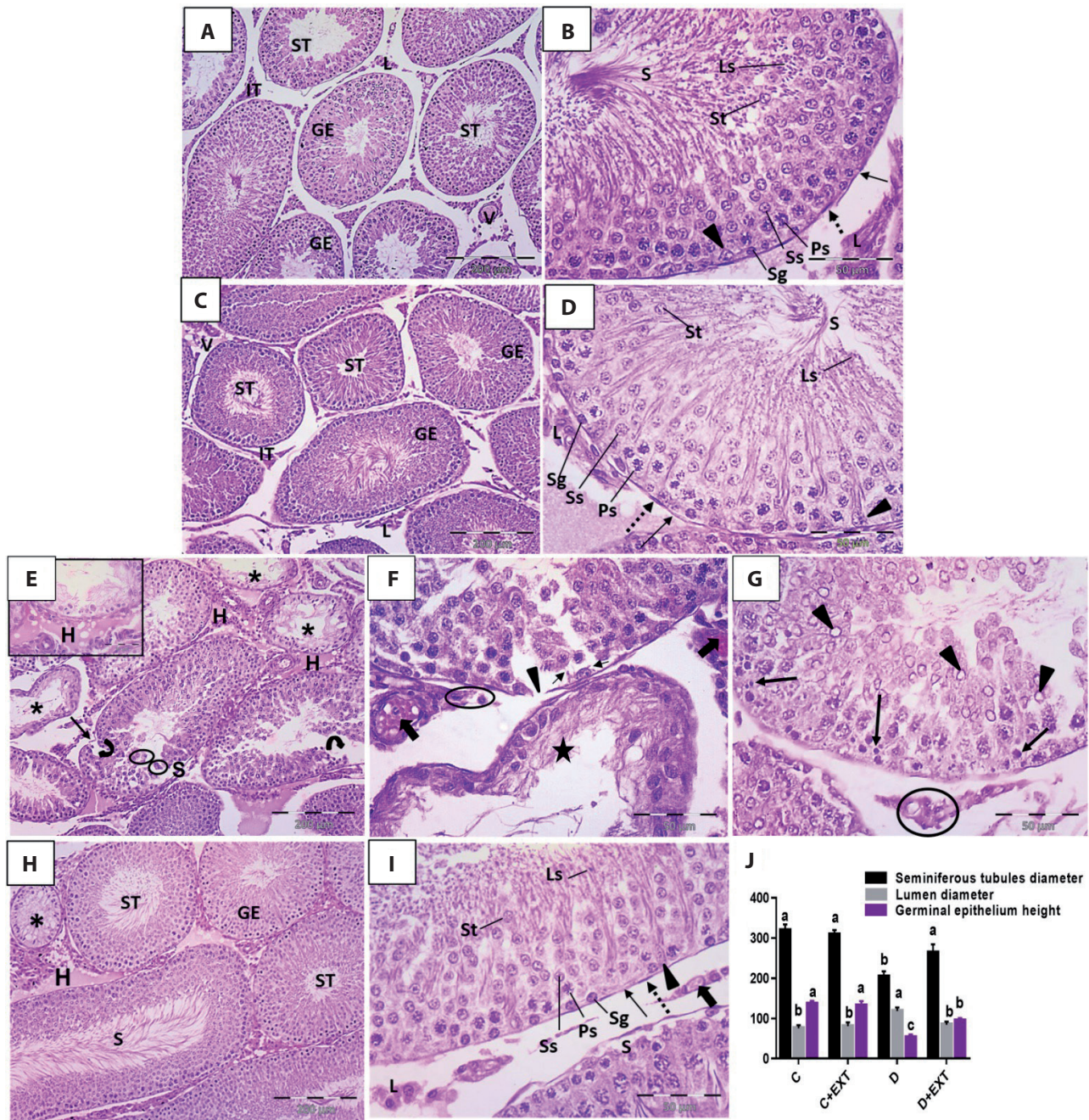


Figure 5. Representative photomicrographs of rat testicular sections of C group (A, B), C+EXT group (C, D), D group (E, F, G) and D+EXT group (H, I). **A, C.** Normal testicular architecture of seminiferous tubules (ST) lined with germinal epithelium (GE). Interstitial tissues (IT) contain leydig cells (L) and blood vessels (V). **B, D.** Germinal epithelium is formed of a series of spermatogenic cells including spermatogonia (Sg), 1ry spermatocytes (Ps) with large nuclei containing dark clumps of chromatin, 2ry spermatocytes (Ss), spermatids (St) with rounded nuclei, late spermatids (Ls) with dense elongated nuclei, and sperm (S) in the tubules' lumina. Sertoli cells (arrowheads) with basally located nuclei and prominent nucleoli, intact basal lamina (arrows) and flattened nuclei of myoid cells (dotted arrows) are noticed. **E.** Some seminiferous tubules are atrophied (*) with depletion of most of the spermatogenic cells and other are distorted with empty spaces within the germinal epithelium (curved arrows), sloughed cells (circles), separation of germinal epithelium from the basal lamina (S) and irregular basal lamina (arrow). Notice the interstitial deposition of acidophilic vacuolated hyaline material (H, inset). **F.** Disturbed architecture of seminiferous tubules (star), discontinuous basal lamina (arrowhead), distorted sertoli cells with disrupted cytoplasmic extensions (arrows) and vascular congestion (thick arrows) with extravascular migration of neutrophils (circle). **G.** Pyknosis (arrows) and karyolysis (arrowheads) of seminiferous tubules lining with degenerated leydig cells (circle).

◀ **H.** Most seminiferous tubules (ST) appear with normal architecture with restoration of germinal epithelium (GE) and sperms (S) in the lumina of most tubules. Scattered atrophied seminiferous tubules (*) and interstitial hyaline deposition (H) are noticed. **I.** Intact germinal epithelium including spermatogonia (Sg), 1ry spermatocytes (Ps), 2ry spermatocytes (Ss), spermatids (St) and late spermatids (Ls) with apparently normal sertoli cells (arrowhead), basal lamina (arrow), myoid (dotted arrow) and leydig cells (L) with minimal vascular congestion (thick arrows). Some seminiferous tubules show separation (S) between basal lamina and germinal epithelium. H&E: magnification $\times 100$ (A, C, E, H), $\times 400$ (B, D, F, G, I). **J.** The mean seminiferous tubule diameter, lumen diameter, and germinal epithelium height (all in μm) of 10 rats in each group are presented in the form of mean \pm SEM. Means having different letters (^{a,b,c}) are significantly different ($p \leq 0.05$). For more abbreviations, see Figure 2.

tion increased the serum level of Kiss that was previously decreased by the use of anabolic androgens, and Oride et al. (2017) who found that the expression of rat hypothalamic Kiss mRNA was significantly increased by GLP-1 administration. Kiss is a hypothalamic neuropeptide that is considered a potent stimulator of the release of gonadotropin releasing hormone (GnRH) (Calley and Dhillon 2014; Dudek et al. 2018). This could explain the improved levels of pituitary gonadotropins seen in this study and, accordingly, testosterone. On the contrary, one study reported contradictory results in which exenatide intervention reduced body weight without increasing the serum level of testosterone in the HFD-induced obese mice. This could

be due to a different model or the duration of the study (Zhang et al. 2015). In addition, administration of exenatide improved sperm count and motility and increased the immuno-expression of vimentin, improving the media required for proper sertoli cell function and spermatogenesis. This is consistent with Zhang et al. (2015), who found that exenatide treatment resulted in a significant rise in sperm motility in HFD fed rats. These results support the testicular protective effects of exenatide in diabetic testis, which could be explained in part by its ability to monitor blood glucose and insulin level in addition to its antioxidant, anti-inflammatory, antiapoptotic and autophagy enhancement effects as reported here.

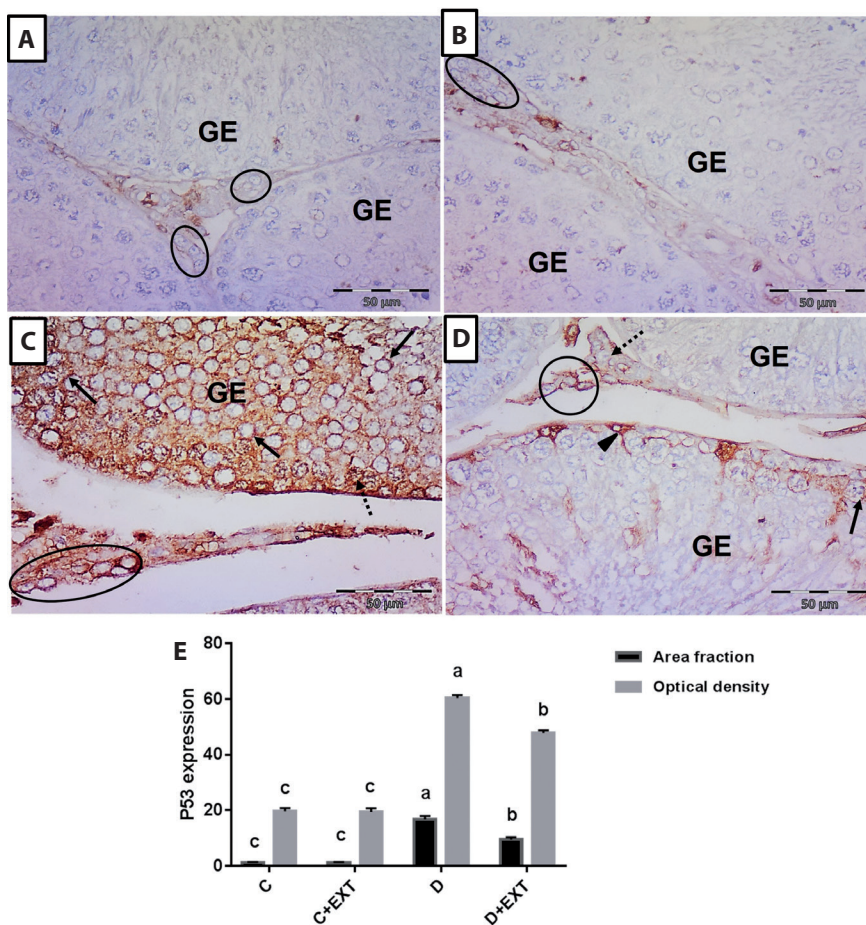


Figure 6. Representative photomicrographs of rat testicular sections immuno-histochemically stained for P53. C group (A) and C+EXT group (B) reveal negative expression in the germinal epithelium (GE) and leydig cells (circles). C. D group exhibits positive expression in the germinal epithelium (GE) mainly cytoplasmic (arrows) with scattered cells having nuclear expression (dotted arrow). Notice leydig cells with positive cytoplasmic expression (circle). D. D+EXT group exhibits negative expression in the majority of the germinal epithelium (GE), with the exception of scattered sertoli cells (arrowhead) and spermatogenic cells (arrow), which exhibit positive cytoplasmic expression. Some interstitial leydig cells show negative expression (dotted arrow) and others show positive cytoplasmic expression (circle). IHC, counterstained with hematoxylin, magnification $\times 400$. **E.** The mean area fraction and optical densities of anti-P53 immuno-positive expression of 10 rats in each group are presented in the form of mean \pm SEM. Means having different letters (^{a,b,c}) are significantly different ($p \leq 0.05$). For more abbreviations, see Figure 2.

Oxidative stress and reactive oxygen species (ROS) have been documented to play a crucial role in diabetic-induced testicular damage with subsequent lipid peroxidation, testicular inflammatory status and apoptosis (Shi et al. 2020). The transcription factor nuclear erythroid factor 2 (Nrf2) has been recognized to play a critical role in the testis. It is documented that decreased expression and/or defective signaling of Nrf2 leads to increased testicular oxidative stress and consequently diabetic testicular damage with defective spermatogenesis. Additionally, Nrf2 has a pivotal role in fighting against oxidative stress by regulating antioxidant enzymes thus increasing the TAC (Yu et al. 2012; Pan et al. 2017).

We found here that Nrf2 expression and the testicular TAC was decreased in the testis of diabetic rats with increased MDA which subsequently led to increased testicular inflammatory status.

The antioxidant effect of exenatide has been shown in other diabetic models (Elbassuoni 2014; Ding et al. 2019), suggesting that the induction of antioxidant enzymes may lie behind exenatide's protective effects and subsequent de-

crease in testicular inflammation. This is consistent with our results which revealed an increase in the nuclear expression of Nrf2. It was reported that Nrf2 performed its function *via* accumulating in the nucleus and inducing cytoprotective enzymes (Li et al. 2013), resulting in increased TAC, IL-10 and decreased TNF- α and MDA testicular levels that were elevated with diabetes.

The role of endoplasmic reticulum stress (ERS) in the pathogenesis of diabetes-induced testicular injury has been reported before (Karna et al. 2020). As seen here, ERS signalling molecules CHOP and caspase-12 were significantly elevated with the induction of diabetes. This is in line with Rashid et al. who documented that ERS was a cause of testicular injury and promoted testicular cell death through up-regulation of pro-apoptotic molecules such as caspase-3, P53 and Bax in diabetic rats (Rashid and Sil 2015). Other studies in diabetic animal models showed activation of testicular oxidative stress and associated p53 signalling and ERS (Zhao et al. 2011; Jiang et al. 2013). All these findings support our results as we found increased immuno-expression of p53 with an increase in the pro-apoptotic Bax and decrease

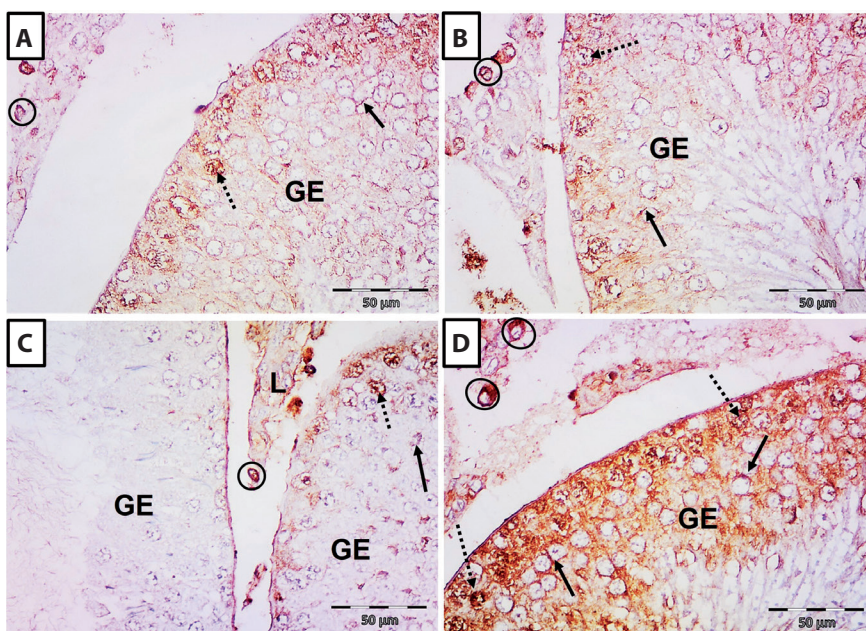
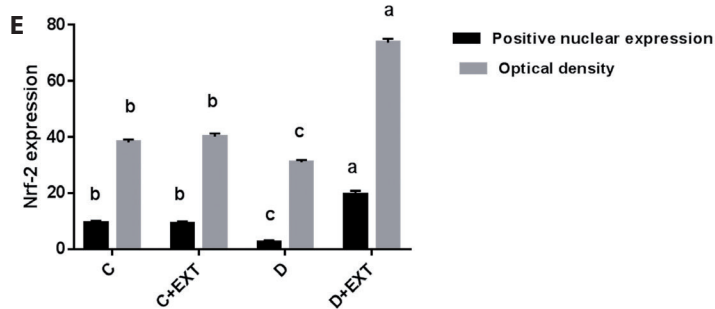


Figure 7. Representative photomicrographs of rat testicular sections immunohistochemically stained for Nrf2. C group (A) and C+EXT group (B) show positive cytoplasmic expression (arrows) in numerous germinal epithelium (GE) cells with scattered cells having positive nuclear expression (dotted arrows). Notice several Leydig cells with positive cytoplasmic expression (circles). C. D group reveals negative expression in most of the germinal epithelium (GE) except for few cells having faint positive cytoplasmic (arrow) or nuclear (dotted arrow) expression. Most of Leydig cells reveals negative expression (L) except for scattered cells with positive cytoplasmic expression (circle). D. D+EXT group reveals strong positive cytoplasmic (arrows) or nuclear (dotted arrows) expression in most germinal epithelium (GE) cells. Many Leydig cells show strongly positive cytoplasmic expression (circles). IHC, counterstained with hematoxylin, magnification $\times 400$. E. The mean numbers and optical densities of anti-Nrf2 positive nuclear expression of 10 rats in each group are presented in the form of mean \pm SEM. Means having different letters (^{a,b,c}) are significantly different ($p \leq 0.05$). For more abbreviations, see Figure 2.



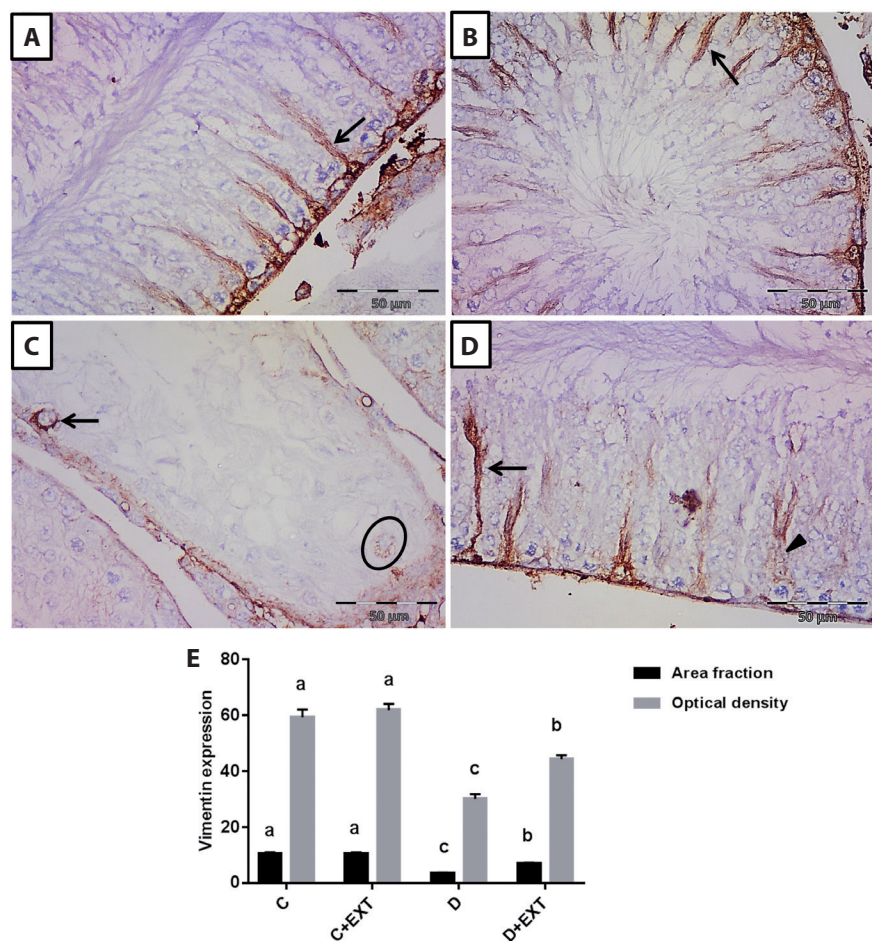


Figure 8. Representative photomicrographs of rat's testicular sections immuno-histochemically stained for vimentin. C group (A) and C+EXT group (B) reveal numerous sertoli cells (arrows) with the normal vimentin filaments distribution, with its characteristic radiating manner toward the seminiferous tubules' lumina. C, D group reveals a few Sertoli cells with positive vimentin staining around the nucleus with collapsed apical extension (arrow). Notice detached Sertoli cell with faint expression (circle). D. D+EXT group showing some Sertoli cells with normal vimentin filaments distribution (arrows) and other with faint expression (arrowhead). IHC, counterstained with hematoxylin, magnification $\times 400$. E. The mean area fraction and optical densities of anti-Vimentin immuno-positive expression of 10 rats in each group are presented in the form of mean \pm SEM. Means having different letters (^{a,b,c}) are significantly different ($p \leq 0.05$). For more abbreviations, see Figure 2.

in the anti-apoptotic Bcl-2 testicular level, which indicates cell apoptosis. An imbalance between Bax and Bcl-2 can activate the downstream apoptotic signalling pathway to induce apoptosis, which ultimately leads to dysfunction of spermatogenesis. Administration of exenatide significantly decreased CHOP and caspase-12 in addition to decreased P53 expression and reversed the levels of both Bax and Bcl-2 denoting its ability to suppress ERS and apoptosis, which share in the improved testicular functions.

Normal autophagy can help to protect against testicular injury caused by hyperglycemia. However, insufficient or immoderate autophagy leads to the degeneration of germ cells and the destruction of organelles such as mitochondria and the endoplasmic reticulum, leading to affection of the testicular normal physiological functions (Shi et al. 2018). Hyperglycemia affects the mTOR and leads to inactivation of autophagy-related genes. Similarly, activation of AMPK is one of the molecular mechanisms that encourages autophagy. It is known that T2DM is characterized by the suppression of AMPK signalling as well as deficient autophagy. These disparities contribute to the increase in

oxidative stress and the development of diabetic complications. This is consistent with our results in which the expression of AMPK was down-regulated in the testicular tissue, which was accompanied by suppressed autophagy reflected by decreased beclin-1 expression and increased mTOR and p62 expression. This is in keeping with Shi et al. (2019) who reported decreased autophagy in testicular tissue of diabetic rats.

Our study demonstrated that apoptosis of testicular tissue in diabetic rats is enhanced in parallel with suppressed autophagy, suggesting a link between them (Zhang et al. 2020). When diabetic rats were treated with EXT, the apoptosis process of testicular injury was effectively repressed, whereas autophagy was enhanced. These findings support the involvement of exenatide's antiapoptotic effect and its ability to augment autophagy in testicular protection against diabetes supporting the role of the AMPK/mTOR signalling pathway in exenatide testicular cytoprotective action.

Notably, it was recorded that GLP-1 can regulate autophagy in different cell types and thereby promotes cell

survival and improve cell function (He et al. 2016; Lim et al. 2016; Arden 2018).

Thus, these intermingled steps linking oxidative stress, ERS, inflammation, autophagy and apoptosis, in which one step leads to the other, contribute to the deterioration of testicular functions by diabetic toxicity, possibly through the AMPK/mTOR/ROS signalling cascade.

Conclusion

Our study proves that GLP-1, besides its ability to manage diabetes, also exerts significant testicular cytoprotective effects. The mechanisms involved may be related to its ability to regulate the AMPK/mTOR/ROS signalling pathway in testicular tissue, thereby regulating autophagy, apoptosis, inflammation, oxidative stress and ERS, resulting in the protection of testicular functions. The results of this study suggest that GLP-1 can exert its protective effects on the testis via a direct impact in addition to correcting hyperglycemia and testicular glucotoxicity. However, more studies are necessary to explore the precise mechanisms underlying the testicular cytoprotective effects of GLP-1.

Compliance and ethical standards. This research protocol was approved by the local ethics committee of Faculty of Medicine, Minia University with approval NO: 146/2021 and was conducted in respect with the NIH guide for care and use of laboratory animals.

Conflict of interest. Authors declare no conflict of interest.

Author contribution to study. All authors declare that all data were generated in-house and no paper mill was used. Abdel-Hakeem EA chose the research point, performed the experiment, collected the results, analyzed the data, wrote and revised the manuscript. Mokhemer SA performed and wrote the histopathology part, immunohistochemistry sections and revised the manuscript. Zenhom NM performed and wrote the RT-PCR analysis. All authors revised the final version of the manuscript and agreed for its publication.

Funding. This research does not receive any financial support.

Data availability. Data is available upon reasonable request from the authors.

References

- Arden C (2018): A role for glucagon-like peptide-1 in the regulation of β -cell autophagy. *Peptides* **100**, 85-93
<https://doi.org/10.1016/j.peptides.2017.12.002>
- Asare-Anane H, Ofori EK, Kwao-Zigah G, Ateko RO, Annan BD, Adjei AB, Quansah M (2019): Lower circulating kisspeptin and primary hypogonadism in men with type 2 diabetes. *Endocrinol. Diab. Metab.* **2**, e00070
<https://doi.org/10.1002/edm2.70>
- Ban K, Noyan-Ashraf MH, Hoefler J, Bolz S-S, Drucker DJ, Husain M (2008): Cardioprotective and vasodilatory actions of glucagon-like peptide 1 receptor are mediated through both glucagon-like peptide 1 receptor-dependent and-independent pathways. *Circulation* **117**, 2340-2350
<https://doi.org/10.1161/CIRCULATIONAHA.107.739938>
- Barakat G, Moustafa ME, Khalifeh I, Hodroj MH, Bikhazi A, Rizk S (2016): Effects of exendin-4 and selenium on the expression of GLP-1R, IRS-1, and preproinsulin in the pancreas of diabetic rats. *J. Physiol. Biochem.* **73**, 387-394
<https://doi.org/10.1007/s13105-017-0565-1>
- Barkabi-Zanjani S, Ghorbanzadeh V, Aslani M, Ghalibafabbaghi A, Chodari L (2020): Diabetes mellitus and the impairment of male reproductive function: Possible signaling pathways. *Diabetes Metab. Syndr.* **14**, 1307-1314
<https://doi.org/10.1016/j.dsx.2020.07.031>
- Calley JL, Dhillo WS (2014): Effects of the hormone kisspeptin on reproductive hormone release in humans. *Advances in Biology* **2014**, 1-10
<https://doi.org/10.1155/2014/512650>
- Caltabiano R, Condorelli D, Panza S, Boitani C, Musso N, Ježek D, Memeo L, Colarossi L, Rago V, Mularoni V (2020): Glucagon-like peptide-1 receptor is expressed in human and rodent testis. *Andrology* **8**, 1935-1945
<https://doi.org/10.1111/andr.12871>
- Castellano JM, Navarro VM, Fernández-Fernández R, Roa J, Vigo E, Pineda R, Dieguez C, Aguilar E, Pinilla L, Tena-Sempere M (2006): Expression of hypothalamic KiSS-1 system and rescue of defective gonadotropic responses by kisspeptin in streptozotocin-induced diabetic male rats. *Diabetes* **55**, 2602-2610
<https://doi.org/10.2337/db05-1584>
- Chang G, Zhang D, Liu J, Zhang P, Ye L, Lu K, Duan Q, Zheng A, Qin S (2014): Exenatide protects against hypoxia/reoxygenation-induced apoptosis by improving mitochondrial function in H9c2 cells. *Exp. Biol. Med.* **239**, 414-422
<https://doi.org/10.1177/1535370214522177>
- Daka B, Langer RD, Larsson CA, Rosén T, Jansson PA, Råstam L, Lindblad U (2015): Low concentrations of serum testosterone predict acute myocardial infarction in men with type 2 diabetes mellitus. *BMC Endocr. Disord.* **15**, 1-7
<https://doi.org/10.1186/s12902-015-0034-1>
- Ding W, Chang W-G, Guo X-C, Liu Y, Xiao D-D, Ding D, Wang J-X, Zhang X-J (2019): Exenatide protects against cardiac dysfunction by attenuating oxidative stress in the diabetic mouse heart. *Front. Endocrinol.* **10**, 202
<https://doi.org/10.3389/fendo.2019.00202>
- Dudek M, Ziarniak K, Sliwowska JH (2018): Kisspeptin and metabolism: the brain and beyond. *Front. Endocrinol.* **9**, 145
<https://doi.org/10.3389/fendo.2018.00145>
- Elbassuoni EA (2014): Incretin attenuates diabetes-induced damage in rat cardiac tissue. *J. Physiol. Sci.* **64**, 357-364
<https://doi.org/10.1007/s12576-014-0327-6>
- Gheibi S, Kashfi K, Ghasemi A (2017): A practical guide for induction of type-2 diabetes in rat: Incorporating a high-fat diet and streptozotocin. *Biomed. Pharmacother.* **95**, 605-613
<https://doi.org/10.1016/j.biopha.2017.08.098>
- Habib HA, Heeba GH, Khalifa MM (2021): Comparative effects of incretin-based therapy on early-onset diabetic nephropathy

- in rats: Role of TNF- α , TGF- β and c-caspase-3. *Life Sci.* **278**, 119624
<https://doi.org/10.1016/j.lfs.2021.119624>
- Hany A, Doaa A, Attia M, Mohammed A (2018): Effect of glucagon like peptide-1 on serum kisspeptin level in adult male albino rats treated by anabolic androgenic steroid. *The Medical Journal of Cairo University* **86**, 1431-1445
<https://doi.org/10.21608/mjcu.2018.56345>
- He Q, Sha S, Sun L, Zhang J, Dong M (2016): GLP-1 analogue improves hepatic lipid accumulation by inducing autophagy via AMPK/mTOR pathway. *Biochem. Biophys. Res. Commun.* **476**, 196-203
<https://doi.org/10.1016/j.bbrc.2016.05.086>
- Heeba GH, Hamza AA (2015): Rosuvastatin ameliorates diabetes-induced reproductive damage via suppression of oxidative stress, inflammatory and apoptotic pathways in male rats. *Life Sci.* **141**, 13-19
<https://doi.org/10.1016/j.lfs.2015.09.015>
- Jiang X, Zhang C, Xin Y, Huang Z, Tan Y, Huang Y, Wang Y, Feng W, Li X, Li W (2013): Protective effect of FGF21 on type 1 diabetes-induced testicular apoptotic cell death probably via both mitochondrial and endoplasmic reticulum stress-dependent pathways in the mouse model. *Toxicol. Lett.* **219**, 65-76
<https://doi.org/10.1088/0004-637X/778/1/65>
- Karna KK, Shin YS, Choi BR, Kim HK, Park JK (2020): The role of endoplasmic reticulum stress response in male reproductive physiology and pathology: a review. *World J. Mens Health* **38**, 484
<https://doi.org/10.5534/wjmh.190038>
- Li Y, Huang Y, Piao Y, Nagaoka K, Watanabe G, Taya K, Li C (2013): Protective effects of nuclear factor erythroid 2-related factor 2 on whole body heat stress-induced oxidative damage in the mouse testis. *Reprod. Biol. Endocrinol.* **11**, 1-10
<https://doi.org/10.1186/1477-7827-11-23>
- Lim SW, Jin L, Jin J, Yang CW (2016): Effect of exendin-4 on autophagy clearance in beta cell of rats with tacrolimus-induced diabetes mellitus. *Sci. Rep.* **6**, 1-15
<https://doi.org/10.1038/srep29921>
- Maresch CC, Stute DC, Ludlow H, Hammes H-P, de Kretser DM, Hedger MP, Linn T (2017): Hyperglycemia is associated with reduced testicular function and activin dysregulation in the Ins2Akita \pm mouse model of type 1 diabetes. *Mol. Cell. Endocrinol.* **446**, 91-101
<https://doi.org/10.1016/j.mce.2017.02.020>
- Mari A, Ahrén B, Pacini G (2005): Assessment of insulin secretion in relation to insulin resistance. *Curr. Opin. Clin. Nutr. Metab. Care* **8**, 529-533
<https://doi.org/10.1097/01.mco.0000171130.23441.59>
- Nazmy WH, Elbassuoni EA, Ali FF, Rifai RA (2019): Proinsulin C-peptide as an alternative or combined treatment with insulin for management of testicular dysfunction and fertility impairments in streptozotocin-induced type 1 diabetic male rats. *J. Cell. Physiol.* **234**, 9351-9357
<https://doi.org/10.1002/jcp.27618>
- Ohkawa H, Ohishi N, Yagi K (1979): Assay for lipid peroxides in animal tissues by thiobarbituric acid reaction. *Anal. Biochem.* **95**, 351-358
[https://doi.org/10.1016/0003-2697\(79\)90738-3](https://doi.org/10.1016/0003-2697(79)90738-3)
- Oride A, Kanasaki H, Mijiddorj T, Sukhbaatar U, Hara T, Tumurbaatar T, Kyo S (2017): GLP-1 increases Kiss-1 mRNA expression in kisspeptin-expressing neuronal cells. *Biol. Reprod.* **97**, 240-248
<https://doi.org/10.1093/biolre/iox087>
- Pan C, Zhou S, Wu J, Liu L, Song Y, Li T, Ha L, Liu X, Wang F, Tian J (2017): NRF2 plays a critical role in both self and EGCG protection against diabetic testicular damage. *Oxid. Med. Cell. Longev.* **2017**, 3172692
<https://doi.org/10.1155/2017/3172692>
- Pujadas G, Drucker DJ (2016): Vascular biology of glucagon receptor superfamily peptides: mechanistic and clinical relevance. *Endocr. Rev.* **37**, 554-583
<https://doi.org/10.1210/er.2016-1078>
- Rashid K, Sil PC (2015): Curcumin ameliorates testicular damage in diabetic rats by suppressing cellular stress-mediated mitochondria and endoplasmic reticulum-dependent apoptotic death. *Biochim. Biophys. Acta* **1852**, 70-82
<https://doi.org/10.1016/j.bbadis.2014.11.007>
- Shi G-J, Zheng J, Han X-X, Jiang Y-P, Li Z-M, Wu J, Chang Q, Niu Y, Sun T, Li Y-X (2018): Lycium barbarum polysaccharide attenuates diabetic testicular dysfunction via inhibition of the PI3K/Akt pathway-mediated abnormal autophagy in male mice. *Cell Tissue Res.* **374**, 653-666
<https://doi.org/10.1007/s00441-018-2891-1>
- Shi W, Guo Z, Yuan R (2019): Testicular injury attenuated by rapamycin through induction of autophagy and inhibition of endoplasmic reticulum stress in streptozotocin-induced diabetic rats. *Endocr. Metab. Immune Disord. Drug Targets* **19**, 665-675
<https://doi.org/10.2174/1871530319666190102112844>
- Shi W, Guo Z, Ji Y, Feng J (2020): The protective effect of recombinant globular adiponectin on testis by modulating autophagy, endoplasmic reticulum stress and oxidative stress in streptozotocin-induced diabetic mice. *Eur. J. Pharmacol.* **879**, 173132
<https://doi.org/10.1016/j.ejphar.2020.173132>
- Srinivasan K, Viswanad B, Asrat L, Kaul C, Ramarao P (2005): Combination of high-fat diet-fed and low-dose streptozotocin-treated rat: a model for type 2 diabetes and pharmacological screening. *Pharmacol. Res.* **52**, 313-320
<https://doi.org/10.1016/j.phrs.2005.05.004>
- Suvarna KS, Layton C, Bancroft JD (2018): Bancroft's Theory and Practice of Histological Techniques. E-Book, Elsevier health sciences
- Tavares R, Escada-Rebello S, Silva A, Sousa M, Ramalho-Santos J, Amaral S (2018): Antidiabetic therapies and male reproductive function: where do we stand? *Reproduction* **155**, R13-R37
<https://doi.org/10.1530/REP-17-0390>
- VanGuilder HD, Vrana KE, Freeman WM (2008): Twenty-five years of quantitative PCR for gene expression analysis. *Biotechniques* **44**, 619-626
<https://doi.org/10.2144/000112776>
- Wang X, Li Z, Huang X, Li F, Liu J, Li Z, Bai D (2019): An experimental study of exenatide effects on renal injury in diabetic rats. *Acta Cir. Bras.* **34**, e20190010000001
<https://doi.org/10.1590/s0102-865020190010000001>
- Yu B, Lin H, Yang L, Chen K, Luo H, Liu J, Gao X, Xia X, Huang Z (2012): Genetic variation in the Nrf2 promoter associates with defective spermatogenesis in humans. *J. Mol. Med.* **90**, 1333-1342

- <https://doi.org/10.1007/s00109-012-0914-z>
Zhang E, Xu F, Liang H, Yan J, Xu H, Li Z, Wen X, Weng J (2015): GLP-1 receptor agonist exenatide attenuates the detrimental effects of obesity on inflammatory profile in testis and sperm quality in mice. *Am. J. Reprod. Immunol.* **74**, 457-466
<https://doi.org/10.1111/aji.12420>
- Zhang K-Q, Tian T, Hu L-L, Wang H-R, Fu Q (2020): Effect of probucol on autophagy and apoptosis in the penile tissue of streptozotocin-induced diabetic rats. *Asian J. Androl.* **22**, 409-413
- https://doi.org/10.4103/aja.aja_89_19
Zhao Y, Tan Y, Dai J, Li B, Guo L, Cui J, Wang G, Shi X, Zhang X, Mellen N (2011): Exacerbation of diabetes-induced testicular apoptosis by zinc deficiency is most likely associated with oxidative stress, p38 MAPK activation, and p53 activation in mice. *Toxicol. Lett.* **200**, 100-106
<https://doi.org/10.1016/j.toxlet.2010.11.001>

Received: September 12, 2022

Final version accepted: October 31, 2022